Quantitative optical determination of the shape of Cu nanocrystals in a composite film

J. Gonzalo,[a)] R. Serna, and C. N. Afonso
Instituto de Óptica, Consejo Superior de Investigaciones Científicas, Serrano 121, 28006 Madrid, Spain

J. Bosbach, T. Wenzel, F. Stietz, and F. Träger
Fachbereich Physik, Universität Kassel, Heinrich-Plett-Strasse 40, D-34132 Kassel, Germany

D. Babonneau
Laboratoire de MétAllurgie Physique, UMR 6630 du CNRS, Université de Poitiers, UFR Sciences, Bat. SP2MI, Bd. 3 Téléport 2, 86960 Futuroscope Cedex, France

D. E. Hole
School of Engineering, Pevensey Building, University of Sussex, Brighton BN1 9QH, United Kingdom

We demonstrate that optical extinction spectroscopy can be used to determine the effective shape of Cu nanocrystals (NCs) embedded in a transparent amorphous Al_2O_3 host both produced by pulsed laser deposition. The axial ratio of the NCs was extracted from the positions of the surface plasmon modes of the optical extinction spectra of the nanocomposite film. Comparison to the results obtained by grazing incidence small angle x-ray scattering shows excellent agreement. Thus, optical spectroscopy can be used as a simple, easily accessible, and versatile tool for the characterization of the NCs that form nanocomposite films. © 2001 American Institute of Physics.
[DOI: 10.1063/1.1362403]

INTRODUCTION

Composite materials containing nanocrystals (NCs) have interesting and potentially useful physical and chemical properties that are different from those of the bulk material.[1–4] This behavior opens up the possibility of fabricating new materials with tailor-made characteristics by exploiting the dependence of the properties of the nanocomposite on the mean size of the NCs. In addition to the size, the *shape* of such NCs also influences the nanocomposite properties considerably.[1–4] For example, nonspherical, metal NCs embedded in insulating materials offer enhanced dielectric and optical properties, making them a credible alternative to existing materials for devices such as integrated polarizers with high extinction ratios[4] or all-optical ultrafast switches with response times of only few picoseconds.[5]

However, precise, easy characterization of metal NCs with nonspherical shapes has been a great challenge in the past in part because of the difficulty to produce such NCs with controlled shapes.[4] It has recently been shown that Cu:Al_2O_3 nanocomposite films grown by pulsed laser deposition have Cu NCs of controlled dimensions and that the use of argon pressure during growth promotes the formation of oblate nanocrystals.[6,7] The objective of the work reported here is to implement optical extinction spectroscopy with polarized light as an easy and efficient means by which to quantitatively determine the effective aspect ratio of oblate NCs in these nanocomposite films. This technique offers several advantages over other methods, the most essential one being its noninvasive character. Furthermore, the method

does not require specially prepared samples like high resolution transmission electron microscopy and it is readily accessible as opposed to grazing incidence small angle x-ray scattering (GISAXS) that requires the use of a large facility.

The method relies on the particular linear optical properties of nanocomposite materials formed by metal NCs embedded in a dielectric matrix whose optical extinction spectra are generally characterized by the presence of large resonances. These resonances are attributed to excitation of plasmon polaritons, i.e., to oscillations of the free electron gas driven by the electromagnetic field, generally referred to as surface plasmon resonances (SPRs).[4,8] The energetic positions, widths, and amplitudes of the SPRs depend on the dielectric functions of the metal of which the NCs are composed and on those of the surrounding material. The optical properties also vary with the size and shape of the NCs. Spherical NCs, that do not interact with each other, exhibit a single resonance whose frequency remains essentially constant for dimensions ($\varnothing$) much lower than the wavelength of the incident light (λ), $\varnothing \ll \lambda$. If the NCs resemble oblate spheroids, i.e., rotational ellipsoids with two main axes $H < \varnothing$, two resonances appear, usually denoted as (1,0) and (1,1) modes. The (1,1) mode results from excitation of the SPR in the direction of the long axis ($\varnothing$) of the NCs whereas the (1,0) mode is brought about by excitation of collective oscillations in the direction of the short axis (H). This behavior also holds for NCs embedded in composites that do not only resemble rotational ellipsoids, but are usually also aligned in the sense that the short axes (H) all point along the direction of the film normal, whereas the long axes ($\varnothing$) lie in the film plane.[9]

[a)]Electronic mail: j.gonzalo@io.cfmac.csic.es

5734

J. Appl. Phys., Vol. 89, No. 10, 15 May 2001

Gonzalo *et al.* 5735

The specific optical response of oblate NCs to the incident electromagnetic field implies that the absorption spectra depend on the polarization of the radiation: *p*-polarized light can excite both the collective electron oscillation parallel [(1,1) mode] and perpendicular [(1,0) mode] to the surface, i.e., in the direction of the long and short axes, whereas *s*-polarized light only stimulates the (1,1) mode.[9] Therefore, the positions of the SPR modes depend on the aspect ratio ($H/\varnothing$) of the NCs, making optical extinction spectroscopy with polarized light an elegant means by which to quantitatively determine the effective aspect ratio of oblate NCs.

EXPERIMENT

Nanocomposite $Cu:Al_2O_3$ thin films were prepared by sequential pulsed laser deposition using an ArF excimer laser beam [$\lambda=193$ nm, $\tau=20$ ns full width at half maximum (FWHM)] operating at 10 Hz. The laser beam was sequentially focused on the surface of high purity Al_2O_3 and Cu targets at an angle of incidence of 45° to lead to an average energy density of ≈ 2 J/cm^2, a value large enough to ablate both targets. The targets were mounted onto a computer controlled holder that provides both continuous rotation of all the targets and sequential ablation of each target. The films were grown at room temperature on Si and glass substrates placed 32 mm from the target surface, either at a base pressure of 1.3×10^{-6} mbar (vacuum) or at Ar pressures of 1.3×10^{-4} and 6.5×10^{-3} mbar.

The reflectivity of the growing film was measured *in situ* and a comparison of it to the calculated expected evolution allowed us to determine the film thickness and effective refractive index.[7] The average deposition rates per pulse of Al_2O_3 and Cu were first determined by growing pure films 100 and 15 nm thick, respectively. A *mass metal thickness* of 1 nm was required to achieve isolated NCs, where the term mass thickness refers to the effective thickness that the film would have if it were a continuous film.[10] The number of laser pulses on each target was selected to produce approximately 20 nm thick Al_2O_3 layers alternated with five layers containing Cu NCs with average dimensions of a few nm.[6,7] As was earlier reported, Ar pressure can be used to change the *in-plane* shape of the NCs.[6,7] This produces a decrease in the average deposition rates compared to those determined in vacuum and thus new calibration specimens were prepared under the gas pressures studied and the number of laser pulses on each target was increased accordingly to achieve films with similar thickness and Cu content. Further details of the synthesis procedure of the nanocomposite films can be found elsewhere.[6,7] Table I summarizes the experimental conditions used to produce the $Cu:Al_2O_3$ films.

Films deposited on Si substrates were analyzed by GISAXS to determine the average dimensions of Cu NCs. The energy was set to 8049 eV, corresponding to a wavelength of 0.154 nm. The distance between the sample and the detector was 650 mm and the angle of incidence was slightly higher than the critical angle of the films ($\alpha \approx 0.22°$) in order to penetrate into the layer.[11] The Cu content in these films was determined by Rutherford backscattering spectrometry (RBS) using a 2.0 MeV ^{4}He$^+$ beam. The backscattered par-

TABLE I. Experimental parameters used to grow the $Cu:Al_2O_3$ nanocomposite films, Cu areal density per layer, and total thickness of the films determined from RBS and RUMP simulations.

Ar pressure (mbar)	No. of pulses in Al_2O_3 per layer	No. of pulses in Cu per layer	Cu areal density per layer ($\times10^{15}$ at./cm^2)	Thickness (nm)
1.3×10^{-6}	1400	150	5.0	136
1.3×10^{-4}	1460	160	7.0	130
6.5×10^{-3}	1700	170	8.5	136

ticles were detected at an angle of 150° and the experimental spectra were simulated using the RUMP program.[12]

The optical extinction spectra of the nanocomposite films deposited on glass substrates were measured under ambient conditions using *p*-polarized light of a Xe arc lamp combined with a monochromator. The photon energies ranged from $E=1.0$ to 5.0 eV and the spectral resolution was $\Delta E=10$ meV. The angle of incidence was 45° with respect to the surface normal of the film. All spectra were corrected for the spectral emission profile of the Xe arc lamp, the wavelength dependent transmission of the optical components, and of the Al_2O_3 films without metal doping as well as for the spectral response of the photodiodes used to detect the light intensity before and after passing through the sample.

RESULTS AND DISCUSSION

The results of the analysis of the film thickness and composition by RBS are summarized in Table I. It is clearly seen that whereas the films have a similar thickness ($\approx 133\pm3$ nm), the Cu areal density is higher in the films grown in Ar pressure than those grown in vacuum. This result indicates that the deposition rate of Cu in Ar is higher than the average estimated value. Scattering of the species ejected from the target by the background gas atoms during the ablation process has been found to produce a decrease in the deposition rate in the pressure range considered in this work ($\leqslant 6.5\times10^{-3}$ mbar). Therefore, the observed behavior is related to processes taking place at the substrate during the early stages of growth. The decrease of desorption/re-emission due to the lower kinetic energy of the species reaching the substrate when deposition takes place in Ar and the formation of nucleation centers in areas where Ar atoms have been adsorbed in the surface have been proposed as possible mechanisms responsible for the increase of the sticking coefficient of the Cu atoms when growth takes place in Ar.[7]

The analysis of the GISAXS patterns obtained for the different films allows the determination not only of the effective values of the in-plane diameter $\langle\varnothing\rangle$ of the NCs but also of their height $\langle H \rangle$ in the direction perpendicular to the film plane and their mean separation $\langle\Delta\rangle$ in the film plane.[6] The values of $\langle\varnothing\rangle$ and $\langle H \rangle$ are shown in Fig. 1 for films grown in vacuum and at the different Ar pressures considered, while the value of $\langle\Delta\rangle$, not shown, was found in all cases to be close to 6 nm. It is seen that the values of $\langle\varnothing\rangle$ increase from 2.8 to 4.0 nm, whereas $\langle H \rangle$ remains close to 2.6 nm for the Ar pressures considered. The $\langle H \rangle/\langle\varnothing\rangle$ ratio,
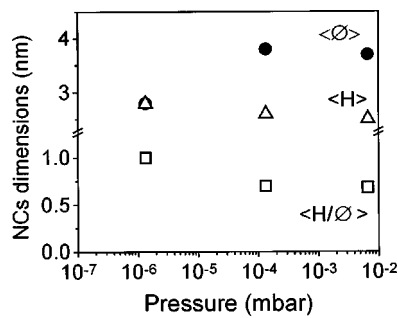
FIG. 1. ● Mean diameter $\langle\varnothing\rangle$ of the Cu NCs in the film plane and ($\triangle$) mean height $\langle H\rangle$ of the NCs in the direction perpendicular to the film plane as a function of the Ar gas pressure used during deposition as determined by GISAXS. ($\square$) Aspect ratio, $\langle H\rangle/\langle\varnothing\rangle$, of the NCs.

FIG. 3. (a) Optical extinction spectra measured with *p*-polarized light at 45° in the Cu:Al$_2$O$_3$ nanocomposite films deposited both in vacuum and at increasing Ar pressures. (b) Calculated extinction spectra using the electrodynamic theory and assuming oblate Cu NCs of constant volume and two different aspect ratios: the solid line is for $H/\varnothing=1$ and the dashed line is for $H/\varnothing=0.7$. The inset in (b) illustrates the meaning of this aspect ratio: H and $\varnothing$ are the height and the mean in-plane diameter of the NCs, respectively.

also shown in Fig. 1, is a measure of the effective aspect ratio of the NCs embedded in the films: values close to 1 mean that the NCs are quasispherical while values below 1 indicate that the NCs are oblate with the long dimension being in the film plane. It is clearly seen in Fig. 1 that the effective aspect ratio is close to 1 for films grown in vacuum whereas it decreases to 0.7 for films grown at 6.5 $\times 10^{-3}$ mbar.

Figure 2 shows the effective in-plane sections calculated from the dimensions of the NCs determined using GISAXS for films grown at the Ar pressures considered. Results obtained from transmission electron microscopy (TEM) analysis of samples prepared under the same experimental conditions, published elsewhere,[7] are included for comparison. As an example, the TEM images corresponding to films grown in vacuum and at 6.5$\times 10^{-3}$ mbar of Ar are shown as insets in Fig. 2. The dark areas in the images, which correspond to the Cu NCs, are embedded in an homogeneous background that corresponds to the Al$_2$O$_3$ host. Previous structural studies using high resolution TEM (HRTEM) of Cu:Al$_2$O$_3$ nanocomposite films grown under similar experimental conditions[13,14] have shown the presence of lattice fringes in the dark areas, thus indicating that the Cu NCs are crystal-

line, whereas the Al$_2$O$_3$ matrix was found to be amorphous. The structural analysis of the samples reported in Ref. 7 showed that the in-plane section of the NCs evolves from circular to elongated when the Ar pressure is increased during deposition. It was also found that the elongated NCs are randomly oriented in the film plane. Thus, the value of $\langle\varnothing\rangle$, calculated from GISAXS patterns, corresponds to an effective diameter of the NCs in the film plane and in this case, the in-plane section was assumed to be circular, with the estimated error being 10%. In the case of data obtained from TEM, an elliptical section was considered to estimate the in-plane section of the Cu NCs using the average sizes reported along the long (L) and short (S) axes of the Cu NCs in Ref. 7: 2.8±0.9 and 2.1±0.4 nm for films grown in vacuum; 3.6±1.5 and 2.3±0.4 nm for films grown at 1.3 $\times 10^{-4}$ mbar of Ar and 6.0±2.9 and 3.1±0.6 nm for films grown at 6.5$\times 10^{-3}$ mbar of Ar. The error is calculated from the statistical deviation of the values for the two axes. It is clearly seen in Fig. 2 that the in-plane section calculated using both methods gives similar values within experimental error and increases as the Ar pressure is increased. We can therefore consider that the $\langle H\rangle/\langle\varnothing\rangle$ ratio shown in Fig. 1 is a good estimation of the effective aspect ratio of the NCs.

Figure 3(a) shows the extinction spectra of films prepared both in vacuum and at the two Ar pressures considered. The SPR of films grown in vacuum and at an Ar pressure of 1.3$\times 10^{-4}$ mbar are well resolved and their peak positions can be easily measured. On the contrary, films grown at the highest Ar pressure considered (6.5 $\times 10^{-3}$ mbar) present a rather broad SPR and thus determination of the SPR peak position is more uncertain. The spectra of films prepared in vacuum exhibit the SPR located at a photon energy of $E=2.2$ eV in addition to an increase of extinction at larger photon energies, typical for the interband transition region of Cu NCs.[4,15] The SPR for films grown in Ar pressure, and thus having anisotropic NCs, is shifted towards lower photon energies, the higher the Ar pressure the larger the shift of the SPR. In both cases the shift is accom-
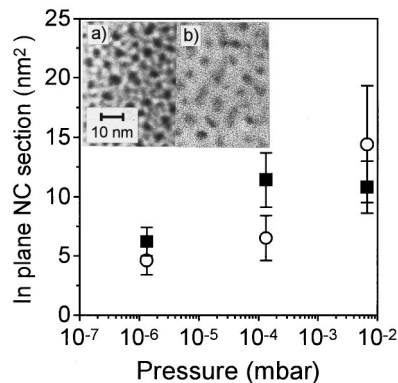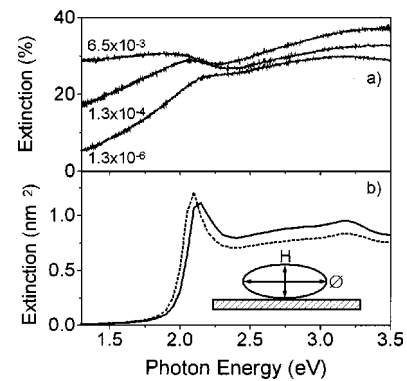

FIG. 2. In-plane section of the Cu NCs as a function of the Ar gas pressure used during deposition calculated from both (■) the $\langle\varnothing\rangle$ determined from GISAXS and (○) the TEM data reported in Ref. 7. The in-plane sections were considered circular and elliptical, respectively. The insets show TEM images of films grown (a) in vacuum and (b) at 6.5$\times 10^{-3}$ mbar of Ar (taken from Ref. 7). The estimated errors in the determination of the in-plane sections are included as error bars.

panied by an increase of the extinction over the whole energy region studied, this increase being consistent with the larger Cu content observed in the RBS experiments for films deposited in Ar pressure (Table I). The broad SPR observed, particularly for those films grown in an Ar environment, is probably related to the broader shape distribution of the NCs,[7] which is responsible for the increasing statistical error in the determination of the average dimensions along the L and S axes, and to the fact that the NCs are randomly oriented in the plane. Nevertheless, only the peak positions of the SPR are relevant to determine the effective aspect ratio of the NCs.

In order to have a quantitative determination of the NCs' aspect ratio from the optical data, the experimental extinction spectra were simulated using electrodynamic theory in the quasistatic approximation.[8] In the model, the NCs are described by rotational ellipsoids with two main axes H and $\varnothing$ as shown in Fig. 3(b), the in-plane section being circular, of diameter $\varnothing$. Electromagnetic coupling among the NCs was neglected in the computations and they were assumed to have the same dielectric function as the bulk material. Although it is known that dielectric functions of metal clusters are size dependent for diameters $\varnothing \lesssim 15$ nm (Ref. 4), resulting in strong broadening of the SPR, the use of the bulk dielectric function is justified here, since the energetic position of the SPR is influenced little by variations of $\varnothing$ for the NCs sizes studied in this work (<10 nm).[4,9] The dielectric function for the Al_2O_3 host has been taken from the data reported elsewhere for pure host films grown by the same technique.[7,16]

The theoretical results obtained for p-polarized incident light and NCs with constant volume and decreasing aspect ratios are shown in Fig. 3(b). The peak positions of the experimentally determined and the theoretically calculated plasmon modes are in reasonable agreement. The resonance at $E = 2.2$ eV calculated for $H/\varnothing = 1$ is brought about by excitation of the SPR in the Cu NCs. Such a single peak is observed in the spectra even for oblate NCs ($H/\varnothing < 1$), since plasmon excitation in Cu NCs is strongly affected by interband transitions.[4] The (1,0) mode is blueshifted compared to the resonance of spherical NCs and thus reaches the energy region of the interband transitions. It is then strongly damped and, therefore, it is not observable in the spectra. In contrast, the (1,1) mode is redshifted for decreasing values of $H/\varnothing$, i.e., away from the interband transition region. Therefore, it does not only appear clearly in the simulated spectra, Fig. 3(b), it even grows in amplitude due to the decreasing influence of the interband transitions. The theoretical curve that matches the position of the maximum of the experimentally determined SPR for the film grown at a pressure of 1.3×10^{-4} mbar leads to an aspect ratio of 0.7 that is in reasonable agreement with the GISAXS data shown in Fig. 1.

In addition to the broad size distribution and the random in-plane orientation of the NCs experimentally observed,[7] other processes such as aggregation,[4] electromagnetic coupling,[4,17] or oxidation[18] (total or partial) of the NCs could account for the non-negligible extinction observed at photon energies lower than 1.8 eV. The first process can be completely discarded from the TEM and GISAXS analysis of the
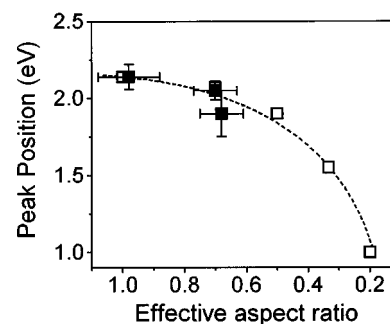

FIG. 4. (■) Experimental and (□) theoretical energy positions of the SPR as a function of the aspect ratio of the Cu NCs. The experimental data are obtained from both Figs. 1 and 3(a), whereas the theoretical data were determined using the electrodynamic theory illustrated in Fig. 3(b). The dashed line is only a guide for the eyes. The horizontal error bars correspond to the estimated errors in the determination of the effective aspect ratio of the NCs from GISAXS measurements, whereas the vertical bars correspond to the uncertainty in the peak position of the SPR.

samples considered in this work. Not only do TEM images (inset in Fig. 2 and Ref. 7) present individual and well isolated NCs, GISAXS spectra also show scattering responses which are only due to isolated NCs, since the mean separation among them, $\langle \Delta \rangle$, presents a very well defined interference effect which is associated with good organization in the plane. The only changes observed in the spectra are those associated with $\langle H \rangle$ and $\langle \varnothing \rangle$, and thus to the anisotropy of the NCs. Moreover, even if the possibility of aggregation could be deduced from the TEM images, it is necessary to take into account the fact that TEM images deal with a very small area of the sample (they are relevant to some hundreds of NCs) while GISAXS measurements are closer to the macroscopic properties of the nanocomposite since they are relevant to values of the order of 10^{10} NCs. The existence of electromagnetic coupling among NCs should also induce a redshift of the SPR as experimentally observed in our case. The scattered fields induced by dipoles is proportional[17] to $(\varnothing/2\Delta^3)$. In the present case $\langle \Delta \rangle \approx 6$ nm for all the films considered whereas $\langle \varnothing \rangle$ evolves from 2.8 to 4.0 nm as shown in Fig. 1. Thus, the proportionality term is at best of the order of $\approx 10^{-2}$ and the coupling among NCs should not be significant. Finally, HRTEM studies of similar nanocomposite films[13,14] have shown that the NCs exhibit lattice fringes consistent with crystalline Cu and, thus, the measured dimensions correspond to metallic Cu NCs. If there is any oxidation of the metal, it would most likely be constrained to a thin shell surrounding the metallic NCs.

Figure 4 shows the dependence of the peak position of the SPR on the effective aspect ratio. The experimental values were determined from Figs. 1 and 3(a) and they correspond to films grown in vacuum and at the two Ar pressures studied. The uncertainty in the peak position of the SPR and the estimated errors in the determination of the effective aspect ratios from GISAXS experiments are included in Fig. 4 as vertical and horizontal error bars, respectively. The calculated position of the SPR for films containing NCs with different aspect ratios are also included for comparison. It is seen that the calculated and experimentally determined data

are in good agreement. The poorest agreement in the case of the film grown at the highest Ar pressure considered ($\approx 6.5 \times 10^{-3}$ mbar) is related to its broader SPR, originated by the observed broader in-plane shape distribution of the NCs[7] and the random in-plane orientation of the NCs previously mentioned. However, the agreement observed for films grown at lower pressures demonstrates the usefulness of optical extinction spectroscopy with polarized light for the determination of the effective shape of embedded NCs.

CONCLUSIONS

We have experimentally demonstrated that the surface plasmon resonance of pulsed laser deposited nanocomposite films formed by Cu NCs embedded in an Al_2O_3 host shifts towards the red when the effective aspect ratio of the NCs decreases as a consequence of an increase in their anisotropy. The shape of the NCs evolved from a near spherical shape (effective aspect ratio ≈ 1) to that of oblate ellipsoids (effective aspect ratio ≈ 0.7), with their short axis being perpendicular to the film plane. The experimentally measured shifts are in reasonable agreement with the ones calculated using the electrodynamic theory in the quasistatic approximation and thus prove that this theory combined with optical extinction spectroscopy measurements can be used effectively to determine the shape of embedded metal NCs.

ACKNOWLEDGMENTS

[1] *Proceedings of the Science and Technology of Atomically Engineered Materials*, edited by P. Jena, S. N. Khanna, and B. K. Rao (World Scientific, Singapore, 1995).

[2] *Small Particles and Inorganic Clusters, ISSPIC 8*, edited by H. H. Anderson (Springer, Berlin, 1997).

[3] *Nanotechnology*, edited by G. Timp (Springer, New York, 1999).

[4] M. Vollmer and U. Kreibig, *Optical Properties of Metal Clusters*, Springer Series in Material Science Vol. 25 (Springer, Berlin, 1995).

[5] R. F. Haglund, Jr., in *Optics of Small Particles, Interfaces and Surfaces*, edited by E. Hummel and P. Wissmuth (Chemical Rubber, Boca Raton, FL, 1996).

[6] J. Gonzalo, R. Serna, J. M. Requejo, J. Solís, C. N. Afonso, and A. Naudon, Appl. Surf. Sci. **154/155**, 449 (2000).

[7] C. N. Afonso, J. Gonzalo, R. Serna, J. C. G. de Sande, C. Ricolleau, C. Grigis, M. Gandais, D. E. Hole, and P. D. Townsend, Appl. Phys. A **69**, S201 (1999).

[8] C. F. Bohren and D. R. Huffman, *Absorption and Scattering of Light by Small Particles* (Wiley, New York, 1983).

[9] T. Wenzel, J. Bosbach, F. Stietz, and F. Träger, Surf. Sci. **432**, 257 (1999).

[10] M. J. Bloemer and J. W. Haus, J. Lightwave Technol. **14**, 1534 (1996).

[11] A. Naudon and D. Thiaudiere, J. Appl. Crystallogr. **30**, 822 (1997).

[12] L. R. Doolitle, Nucl. Instrum. Methods Phys. Res. B **9**, 344 (1985).

[13] J. M. Ballesteros, R. Serna, J. Solís, C. N. Afonso, A. K. Petford-Long, D. H. Osborne, and R. F. Haglund, Appl. Phys. Lett. **71**, 2445 (1997).

[14] C. N. Afonso, R. Serna, J. M. Ballesteros, A. K. Petford-Long, and R. C. Dooler, Appl. Surf. Sci. **127–129**, 339 (1998).

[15] K. Uchida, S. Kaneko, S. Omi, C. Hata, H. Tanji, Y. Asahara, and A. J. Ikushima, J. Opt. Soc. Am. B **11**, 1236 (1994).

[16] R. Serna, J. C. G. de Sande, J. M. Ballesteros, and C. N. Afonso, J. Appl. Phys. **84**, 4509 (1998).

[17] Z. Liu, H. Wang, H. Li, and X. Wang, Appl. Phys. Lett. **72**, 1823 (1998).

[18] G. De, M. Gusso, L. Tapfer, M. Catalano, F. Gonella, G. Matei, P. Mazzoldi, and G. Battaglin, J. Appl. Phys. **80**, 6734 (1996).